Local thickness computation in 3D meshes and 3D printability assessment

Celestin Lanterne, Stefka Gueorguieva, Pascal Desbarats

LOCAL THICKNESS COMPUTATION IN 3D MESHES AND 3D PRINTABILITY ASSESSMENT

Celestin Lanterne* **, Stefka Gueorguieva* and Pascal Desbarats*
*University of Bordeaux,
351, Cours de la Libération, 33405 Talence
**FabZat,
120, Ave de Maréchal Leclerc, 33130 Bègles

ABSTRACT

We present an approach to printability assessment of 3D meshes depending on shape's local thickness measure.
We propose a method for detection of regions with critical thickness based on volume bracketing. Our method is conceived as a designer assistance tool and can be iterated until the structural soundness is achieved.

KEYWORDS

3D printing, structural analysis, model repair, polygonal mesh

1. INTRODUCTION

Digital object representations used as input data in rapid prototyping work flows should fulfill design and fabrication constraints that ensure the manufacturing of solid prototypes. These constraints can be analyzed in a twofold sense: as geometry and topology requirements related to the definition of an object with well identified interior and exterior volume, and structural weakness requirements related to the 3D printability assessment and the lack of critical features that can damage the integrity of the manufactured prototype.
There is a great variety of mesh repairing methods [21,2] that fix up errors in geometry and topology structure and transform input mesh into watertight manifold surface [9,7]. Unlike mesh repairing, printatiblity assessment is a more recent domain of investigations, growing considerably along with the ubiquitous 3D printing applications such as stress analyzing [18,24,15], heterogeneous material object fabrication [5], model balancing [17], printing of articulated models [8], partitioning into printable parts [14].
Structural weakness control is related to the 3D local thickness. In computational geometry, shape thickness is broadly used for surface shape extraction [6], reconstruction [1,16] and skeletonization [10,13,20,19]. Thickness control is the result of complex structural optimization computations [4] and the optimal shape is not manufacturable by standard rapid prototyping work flows.
The purpose of this paper is to present a simple and practical method for 3D printability assessment based on local thickness evaluation of meshes that include portions of not watertight surfaces often encountered in industrial applications. Depending on the critical threshold of manufacturability, surface wall thickness is corrected through an user interaction interface ameliorating the solidity of the prototype.

2. RELATED WORKS

Methods for local thickness estimation can be classified into two categories, surface-based and volume-based, depending on the local structure thickness in use. Following the surface-based approach, local thickness is defined for every point on the surface as a measure of the distance to the "opposite" surface. Jones et al. [12] , for example, propose a measure of the brain cortical thickness. The volume of the cortex is

represented as the domain for the solution of the Laplace's equation ($\nabla^2\psi=0$) with boundary conditions at the gray-white junction and the gray-CSF junction. Normalized gradients of ψ define a vector field with vectors tangent to field lines connecting both boundaries. The cortical thickness for a given point of the cortex is defined as the path length along the field line that passes through the point and connects the opposite boundary. The key advantage of this definition is that thickness is uniquely defined for any point in the cortex.

The volume based approach can be illustrated by the method of Hildebrand et al. [11] that estimates local thickness by fitting maximal spheres to every point in the structure. The local thickness at a given point is defined as the diameter of the largest sphere which contains the point and which is completely inside the structure. The model-independence is the basic advantage of this method. It can easily quantify the variability of the thickness and facilitates remodeling undergoing structure. Unfortunately, there is a loss of reciprocity and uniqueness of thickness measure.

The above methods estimate local thickness independently of the downstream applications. Considering 3D printing technology in use, local thickness can be defined in a more technology dependent way. For layered manufacturing for example [3], selecting the build direction resolves some problems in local wall thickening of open contoured surfaces.

3. OUR APPROACH

We are interested in printability assessment of input model that is composed by different connected components, enclosing volumes or being flat, with possible encapsulations, intersections and missing boundaries. Shape thickness can be associated to the measure of the distance between component boundaries that define the limit between the empty space and the solid material. The basic idea is to use a ray tracing algorithm to compute the local thickness as the distance between the pair of “opposite” boundaries.

Algorithm 1: Local thickness computation in 3D Mesh

Input: Triangle mesh T

Output: $T[]=\{thickness_{fT}\}$, $\forall f_T, f_T \in T$, $thickness_{fT}$ measure of local thickness for f_T

begin
  for $\forall f_T, f_T \in T$ **do**
    Trace r_{fT}, through the geocenter of f_T and opposite to the normal of f_T;
    for $\forall f, f \in T \wedge f \neq f_T$ **do**
      Compute $D_{fT}[f], D_{fT}[f] = (inter_f, dist_f, orient_f)$;
      if $r_{ft} \cap f \neq 0$ **then**
        $inter_f$ = true ; $dist_f$ = the distance from the geocenter of f_T to f along r_{fT} ;
        $orient_f$ = -1 if r_{fT} has the same direction as the normal of f else $orient_f$ = 1 ;
      else
        $inter_f$ = false ; $dist_f = \infty$; $orient_f = \infty$;
      endif
    done
  Compute $T[f_T], T[f_T] =$ **LTC**(f_T, D_{fT});
  done
end

Let T denotes the input model. For each face f_T, $f_T \in T$, a ray r_{fT} is traced through the geocenter and opposite to the face normal. Crossing points between the ray and the input model are computed. To each crossing point a bracket, left or right, is associated depending on whether the ray "enters" or "leaves" the model component according to the normal orientation of the intersected face. Thus, along the ray, a bracketing expression is constructed. We check for balanced brackets in this expression. Local thickness is defined as the distance between the crossing points corresponding to the first left bracket and the matching right bracket. We denote the above processing as a whole like "volume bracketing".
The Algorithm 1 iterates on each face of the input model in two steps. First, a preprocessing phase to compute information necessary to volume bracketing, and second, given by Algorithm 2, the construction and the evaluation of the volume bracketing expression.

Algorithm 2: **LTC**(f_T ,D_{fT})

Input: Face f_T , $f_T \in T$, $D_{fT}[] = \{ (inter_f , dist_f , orient_f) \}$, $\forall f, f \in T \wedge f \neq f_T$

Output: thickness f_T

begin
Let $IntExt$ = 1 and $FindExt$ = false ;
Sort $D_{fT}[]$ in increasing order according to $dist_f$;
for all $d \in D_{fT}[]$ **do**
if $d.inter_f$ = = true **then**
$IntExt$ += $d.orient_f$;
if $IntExt$ = = 0 $\wedge$ $FindExt$ = = false **then**
$FindExt$ = true ; $thickness_{fT}$ = $d.dist_f$;
endif
endif
done
if $IntExt \neq 0$ **then** $thicknessf_T$ = false; **endif**
end

Figure 1:(a,b,c) Local thickness evaluation. (d) Evaluation failure for internal face f_T, , $f_T \in \partial A \wedge f_T \in B$.(e) Evaluation failure for unbounded model.

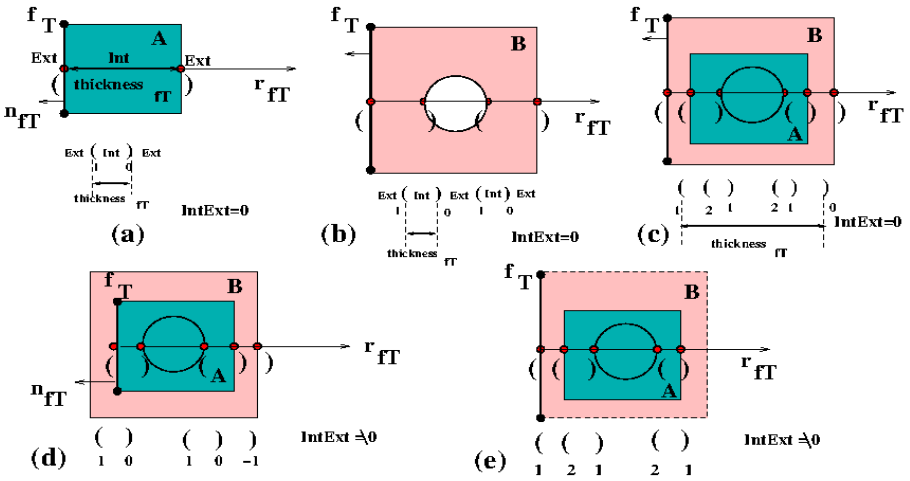

In Figure 1, a two dimensional case is illustrated. For the example Figure 1(a), the input is a component A with simple connected boundary ∂A. The ray r_{fT} crosses ∂A, in a single point. A left bracket is associated to the geocenter as long as r_{fT} "enters" into A, and a right bracket is associated to the intersection point, as long as r_{fT} "leaves" A. Checking for balance in the expression is simply associated to a counter $IntExt$, incremented by one when crossing a left bracket, and decremented by one, when crossing a right bracket. At the geocenter, $IntExt$ is initialized to one. The thickness is measured when $IntExt$ is annulled for the first time. The scan of the crossing points continues all over the ray r_{fT}. The thickness calculation is valid only if at the end, $IntExt=0$. A component with a hole is shown in Figure 1(b). When the initial face belongs to an internal shell, Figure 1(d), or in some cases when the input mesh includes missing boundaries, Figure 1(e), the algorithm fails. Cases when faces do not support a valid computation of the local thickness are left for post processing. Indeed, the computation failure indicates the presence of errors or biases in the input model that should be fixed before re-iterating the computation.

4. RESULTS

All prototypes are produced on a “Z-Corp” printer with a height of 7 cm. First, we illustrate an example of printability assessment based on Kate's model. The input mesh, shown in Figure 2(a), is a multi-shell model with intersections and flat surfaces. The evaluation of the local thickness is given in Figure 2(b) and the 3D printing is shown in Figure 2(c). It can be seen that regions with critical thickness, as the right hand and the belt, are detected by the volume bracketing algorithm. In the first case, the designer corrects the critical thickness by attaching the hand to the hip thus avoiding hand's break during printing. In the second case, the critical region is left unchanged that produces a crack in the prototype.

Figure 2: (a) Kate's mesh model (b) Local thickness evaluation (c) Kate's prototype.

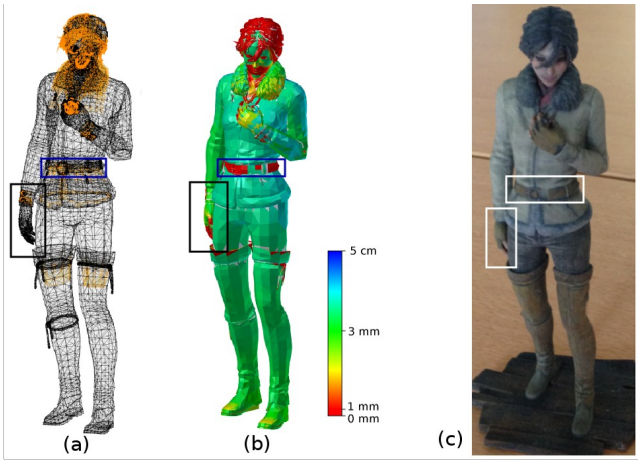

In Figure 3 we give thickness evaluation by volume bracketing on commonly used test models [15,18,22,23,24]. The results of the 3D printing are shown in Figure 4. As expected arms and legs of banana man break on printing as pointed by their critical local thickness. The support of the soccer cup is built in six strips. Despite of the critical thickness of each individual strip, the prototype preserves its integrity. In contrast, hanging ball does not contain regions with critical thickness but the gravity of the ball cut off the connection to the shelf. Lastly, the shell is of uniform thickness as does the corresponding prototype that

remains in a single piece. These experiments show that volume bracketing provides correct evaluation of the local thickness. Our method supplies a simple and fast feedback on the printability of the input models but is less precise than structural analysis supported by multi-objective optimization and mechanics analysis. For example, in comparison with stress analysis of Stava et al. for the shell model shown in Figure 3(e), illustration issued from [18] Figure 5, volume bracketing produces uniform thickness and does not take into account structural weakness ought to gravity and stress. Besides the fact that there is good probability for prototype to break in regions with critical thickness, additional structural weakness constraints are needed to fully determine printability assessment.

Figure 3: Local thickness evaluation (a) Banana man (b) Soccer cup (c) Hanging ball (d) Shell.

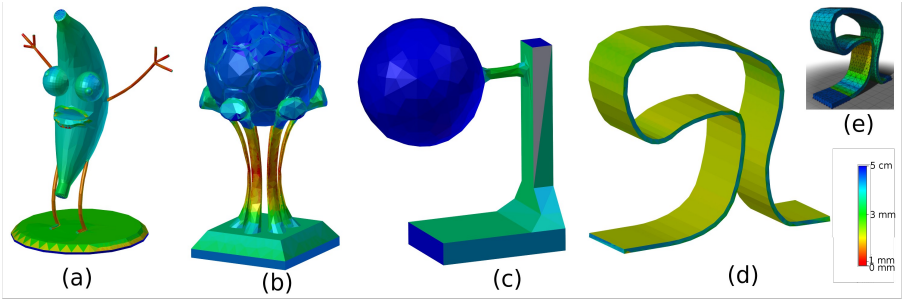

Figure 4:Prototypes of test models produced on a "Z-Corp" 3D printer.

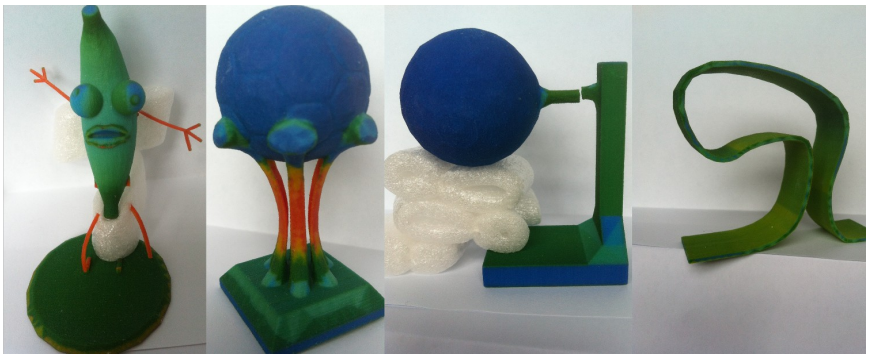

5. CONCLUSION

Printability assessment of mesh models is related to the structural soundness and weakness control on input date. In the present article, we propose a method for detection of regions with critical thickness based on volume bracketing. The method is used for local thickness evaluation of meshes with available face normal orientation. The elaborated method is implemented and experienced in an industrial 3D prototyping chain as an interactive designer assistance tool. The experimental results are economically viable in comparison with the classical work flows based on the watertight surface reconstruction as a preprocessing step that is time consuming, computationally expensive and possibly error-prone. The provided industrial feedback implies further case study for errors to be repaired before prototype manufacturing and deeper understanding of the physical constraints. Our goal is to reduce as much as possible interaction during mesh repairing while maintaining the initial designer concept.

ACKNOWLEDGEMENT

This work is supported by ANRT, the Association of National Research and Technology, The Industrial Agreements for Training through Research (CIFRE) grant, FabZat SAS Company. We thank F. Pitoun and D. Chevalier for triggering this research, providing us with 3D printing support.

REFERENCES

[1] Amenta, N. et al., 2001. The power crust, unions of balls, and the medial axis transform. *Comput. Geom.*, Vol. 19, No. 2-3, pp. 127-153.

[2] Attene, M. et al., 2013. Polygon mesh repairing: An application perspective. *ACM Comput. Surv*., Vol. 45, No. 2, pp. 15.

[3] Alexander, P. and Dutta, D., 2000. Layered manufacturing of surfaces with open contours using localized wall thickening. *Computer-Aided Design*, Vol. 32, No. 3, pp. 175-189.

[4] Allaire,G. And Jouve, F., 2008. Minimum stress optimal design with level set method. *Engineering analysis with boundary elements*, Vol. 32, No. June, pp. 909-918.

[5] Bickel, B. et al., 2010. Design and fabrication of materials with desired deformation behavior. *ACM Trans. Graph.*, Vol. 29, No. 4, pp 63:1-63:10.

[6] Blum, H. and Nagel, R. N. ,1978. Shape description using weighted symmetric axis features. *Pattern Recognition*, Vol. 10, No. 3, pp. 167-180.

[7] Berger, M. and al., 2014. State of the art in surface reconstruction from point clouds. *Eurographics*, Strasbourg, France, pp. 161-185.

[8] Cali, J. and al., 2012. 3D-printing of non-assembly, articulated models. *ACM Trans. Graph*,, Vol. 31, No. 6, pp. : 130:1-130:8

[9] Dey, T.K. and Goswami,S., 2003. Tight cocone: A water-tight surface reconstructor. J. *Comput. Inf. Sci. Eng.*, Vol. 3, No. 4, pp. :302—307.

[10] Dey, T.K. and Sun, J. , 2006. Defining and computing curve-skeletons with medial geodesic function. Proceedings *of the Fourth Eurographics Symposium on Geometry Processing*, Cagliari, Sardinia, Italy, pp. 143-152.

[11] Hildebrand, T. and Rüegsegger, P., 1997.A new method for the model-independent assessment of thickness in three-dimensional images. *Journal of Microscopy*, Vol. 185, No. 1, pp. 67-75.

[12] Jones, S.E. and al., 2000. Three-dimensional mapping of cortical thickness using Laplace's equation. *Human Brain Mapping*, Vol. 11, No. 1, 12-32.

[13] Ju, T. and al., 2007. Computing a family of skeletons of volumetric models for shape description. *Computer-Aided Design*, Vol. 39, No. 5, pp. 352-360.

[14] Luo, L. and al., 2012., Chopper: partitioning models into 3d-printable parts. ACM Trans. Graph., Vol. 31, No. 6, pp. : 129:1-129.9.

[15] Lu, L. and al., 2014. Build-to-last: strength to weight 3d printed objects. *ACM Trans. Graph*., Vol. 33, No. 4, pp. : 97:1-97:10.

[16] Petitjean, S. and Boyer, E., 2001. Regular and non-regular point sets: Properties and reconstruction. *Comput. Geom.* Vol. 19, No. 2-3, pp. :101-126.

[17] Prévost, R. and al., 2013. Make it stand: balancing shapes for 3d fabrication. *ACM Trans. Graph*, Vol. 32, No. 4, pp. :81:1-81:10.

[18] Stava, O. and al., 2012. Stress relief: improving structural strength of 3D printable objects. *ACM Trans. Graph*., Vol. 31, No. 4, pp.48:1-48:11.

[19] Sobiecki, A. and al., 2013. Qualitative comparison of contraction-based curve skeletonization methods. *Mathematical Morphology and Its Applications to Signal and Image Processing*, 11th International Symposium, Uppsala, Sweden, pp. 425-439.

[20] Telea, A. and Jalba, A., 2012. Computing curve skeletons from medial surfaces of 3d shapes. *Theory and Practice of Computer Graphics*, Rutherford, United Kingdom, pp. 99-106.

[21] Tu, J., 2009. Fixing geometric errors on polygonal models: A survey. *J. Comput. Sci. Technol*., Vol. 24, No. 1, pp 19-29.

[22] Umetani, N. and Schmidt, R. , 2013. Cross-sectional structural analysis for 3d printing optimization. *SIGGRAPH Asia*, Hong Kong, China, November, pp. 19-22

[23] Wang, W. et al., 2013, Cost-effective printing of 3d objects with skin-frame structures. *ACM Trans. Graph*., Vol. 32, No. 6, pp. 177:1-177:10.

[24] Zhou, Q. and al., 2013. Worst-case structural analysis. *ACM Trans. Gr.*, Vol. 34, No. 4, pp. 137:1-137:12.